SF2A 2016
C. Reylé, J. Richard, L. Cambrésy, M. Deleuil, E. Pécontal, L. Tresse and I. Vauglin (eds)

CONSEQUENCES OF ROTATING OFF-CENTRED DIPOLAR ELECTROMAGNETIC FIELD IN VACUUM AROUND PULSARS

A. Kundu[1] and J. Pétri[1]

Abstract. Studying the electromagnetic field of pulsars is one of the key themes in neutron star physics. While most of the works assume a standard central dipolar electromagnetic field model, recently some efforts had been made in explaining how inclusion of higher field components produces drastic consequences in our understanding of these objects.

We put forward the effects of a unique recently presented approach in which the magnetic axis is shifted off from the centre. It is found that the rotating off-centred dipolar electromagnetic field itself reveals the presence of the higher components within. The consequences of this approach on the shape of the polar caps and the emission diagrams are discussed.

Keywords: dipole, magnetic fields, neutron stars, pulsars, off-centred

1 Introduction

Pulsars are a special class of neutron stars (Gold (1968)) with strong magnetic fields and rotation period lying between 1.4 ms and 8.5 seconds. Since their discovery (Hewish et al. (1968)), several attempts have been made to understand these mysterious objects. The magnetic field topology of pulsars provides insight into the physical processes and hence, extensive literature focusses on it.

A simple model for the magnetic poles and the magnetic field line structure was put forward by Radhakrishnan & Cooke (1969) and the electromagnetic field equations for a rotating dipole in vacuum were first presented by Deutsch (1955) giving the symmetrical solutions about a magnetic dipole which is inclined to the rotation axis. Most of the followed literature is focussed on these standard assumptions.

However, with the discovery of pulsar J2144-3933 which have a period of 8.51 s, by far the longest of any known radio pulsar, it was realized that this simple assumption needs revision (Young et al. (1999)). It was argued by Gil & Mitra (2001) that to explain this extremal observation, a complicated multi-polar surface magnetic field has to be considered. Gil et al. (2002) modelled surface magnetic field of neutron stars which required strong and non-dipolar surface magnetic field near the pulsar polar cap. The electromagnetic field was considered by them to be a superposition of the global dipole field and a small scale magnetic anomaly. Petri (2015) included multipolar components to the electromagnetic field in a self-consistent way and demonstrated that working with only a dipole field can be very misleading.

It is also assumed by default that the centre of the magnetic dipole coincides with the centre of the rotation axis. However, it has been shown that a deviation from this centred assumption i.e. an off-centred geometry is possible for stars and planets by Stift (1974) and Komesaroff (1976) respectively. The offset idea was applied to the neutron stars by Harding & Muslimov (2011) to investigate the effects of offset polar caps on pair cascades near the surface. Recently, Petri (2016) studied the effect of an offset dipole anchored in the neutron star interior and calculated exact analytical solutions for the electromagnetic field in vacuum outside the star. We use these equations to study the consequences of the off-centred approach.

[1] Observatoire Astronomique de Strasbourg, Université de Strasbourg, CNRS, UMR 7550,
11 Rue de l'université, F-67000 Strasbourg, France

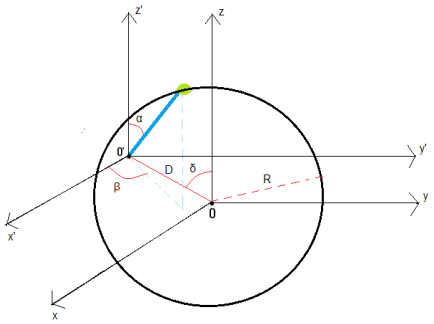

Fig. 1: Geometry of an off-centred Pulsar

2 Off-centred geometry

Figure 1 depicts the geometry of an off-centred pulsar of radius R. The centre of the unprimed reference frame xyz coincides with the geometrical centre O of the pulsar. Hence, this is the frame which is attached to the rotation axis of the pulsar. The position vector for a random vector in this centred frame is defined as $\mathbf{r} = r\mathbf{n}$ where $\mathbf{n} = (\sin\theta\cos\phi, \sin\theta\sin\phi\cos\theta)$.

We define another reference frame $x'y'z'$ attached to the magnetic axis of the pulsar which is centred at O'. The centre of this new frame O' is shifted from O by a distance D. Let's call this primed reference frame $x'y'z'$ as the off-centred frame.

The angle of inclination between the two frames w.r.t. the $z - axis$ of the centred frame is δ. The magnetic axis is shown in blue with polar angle and azimuth angle as α and β respectively as seen from the off-centred frame. It is defined as $\mathbf{m} = m(\sin\alpha\cos\beta, \sin\alpha\sin\beta, \cos\alpha)$ and its position vector w.r.t. the centred frame is given by $\mathbf{d} = D(\sin\delta, 0, \cos\delta)$

An important condition used throughout the calculations was $D << R$ as the centre of the magnetic axis must lie within Pulsar. A quantity $\epsilon = D/R$ was defined and hence, we have, $\epsilon << 1$. The angles α, β and δ are shuffled to get different orientations for the off-centred geometry. We chose $\epsilon = 0.2$ for the off-centred calculations throughout the discussion.

3 Results and Discussions

The exact analytical expressions for dipolar and quadrupolar electromagnetic fields recently published in Appendix C of Petri (2016) are used for all the calculations.

3.1 Polar cap geometry

Polar cap is the region mapped out by the foot points of the magnetic field lines touching the light cylinder. Studying polar caps is considered crucial to understand the pulsar radio emission as this is the region which is most likely to be the source of the coherent radio emission. We present a comparison of the polar cap geometry for the centred and the off-centred geometry.

The comparison is shown in Figure 2 where we plot the shapes of the polar caps for various inclination angles. The x and y axis represent the azimuth angle ϕ and the polar angle θ respectively. The centred case (shown in green) has been calculated by considering $\epsilon = 0$ and for the off-centred case (shown in blue) ϵ is taken to be 0.2.

A broad view distinction depicts that the shape is not affected due to the shift of the centre of the dipole from the geometrical centre but size, apparently, is affected. The size of the polar cap is one of the determining factors for the pulse profile width of pulsar. The larger polar caps as evident in (b) could be used to justify observations with longer pulse widths than expected.

The shift in the location of the polar caps in terms of θ for aligned geometries defined by $\delta = 0$ are seen in parts (a) to (d) of the Figure 2.

In contrast to the aligned case, the orthogonal geometries defined by $\delta = 90$ show a shift in ϕ. The shift for each pole is in opposite directions as seen in (e) and (f). This shift in ϕ represents a phase delay which could

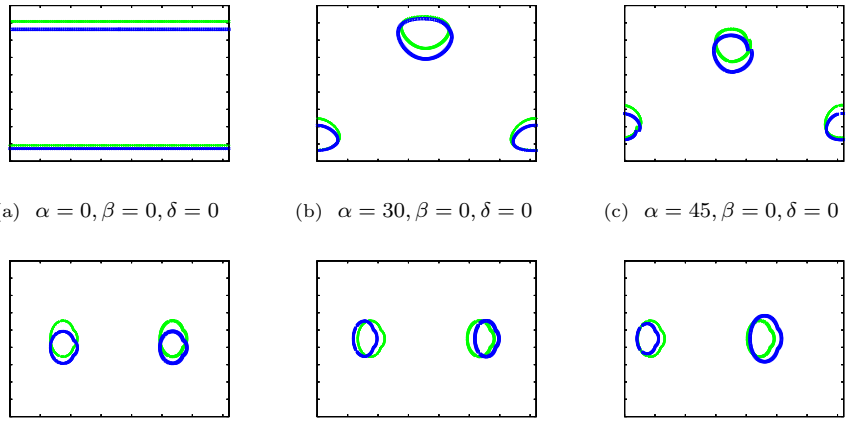

(a) $\alpha = 0, \beta = 0, \delta = 0$ (b) $\alpha = 30, \beta = 0, \delta = 0$ (c) $\alpha = 45, \beta = 0, \delta = 0$

(d) $\alpha = 90, \beta = 90, \delta = 0$ (e) $\alpha = 90, \beta = 90, \delta = 90$ (f) $\alpha = 90, \beta = 45, \delta = 90$

Fig. 2: Polar cap geometry comparison for $\epsilon = 0$ (in green) and $\epsilon = 0.2$ (in blue) for various cases

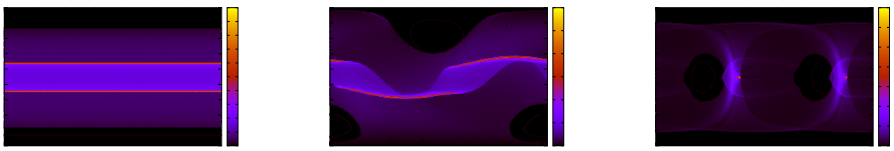

(a) $\alpha = 0, \beta = 0, \delta = 0$ (b) $\alpha = 30, \beta = 0, \delta = 0$ (c) $\alpha = 90, \beta = 90, \delta = 90$

Fig. 3: High energy emission phase diagrams for $\epsilon = 0.2R$ for various cases

serve as a crucial factor to compare observational phase delays in pulse profiles with our approach and hence, explain such observations.

3.2 High energy emission phase diagrams

We present the phase diagrams for the high enery emission in this section.

In Figure 3 we show the high energy emission for a shift of $\epsilon = 0.2R$ for several cases. The $x - axis$ spans the phase ϕ while the $y - axis$ represents the angle of the line of sight. The key on the right side of each plot represents the intensity. The black region corresponds to the no emission region and moving towards yellow means an increase in the photon count. For all the three cases shown we see the black region close to the poles which specifies the 'no emission' zone. It is in accord with the theory that the high energy emission has its source close to the light cylinder. It is not very easy to precisely conclude things related to the off-centred approach from these phase diagrams so we will plot the light curves in the next section. We also show the light curves for the radio emission.

3.3 High energy emission and radio emission light curves

To understand the phase diagrams deeply we need to have a look at the higher resolution which can be attained by extracting light curves from them.

Light curves for high energy and radio regime for $\alpha = 30, \beta = 0, \delta = 0$ and $\alpha = 90, \beta = 90, \delta = 90$ are shown in Figure 4 and Figure 5 respectively.

We see clearly the radio emission complements the high energy emission with the former being the strongest at the poles and the latter in proximity to the light cylinder.

In (a), (b) and (d) parts of Figure 4 we see that the pulse width varies for the two regimes. In (c) it can be noticed that the high energy emission is spread over almost entire range of ϕ, we do not see a dip close to zero in Figure 4 but we have very clear such dips in the orthogonal case in Figure 5 which is entirely based on

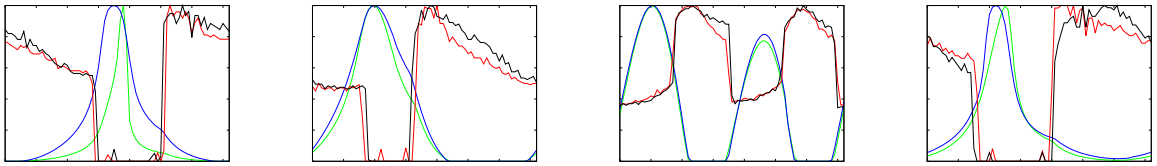

(a) $\theta = 30$ (b) $\theta = 45$ (c) $\theta = 90$ (d) $\theta = 150$

Fig. 4: High energy and radio emission light curves for $\alpha = 30, \beta = 0, \delta = 0$ with $\epsilon = 0$ and $\epsilon = 0.2R$ for various line of sight angles. The high energy emission curves are shown in red and black for the centred and the off-centred case respectively. Similarly, the green and the blue curves represent the emission curves for the radio regime in the same order.

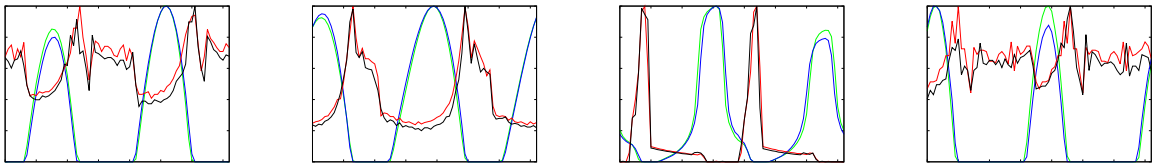

(a) $\theta = 30$ (b) $\theta = 45$ (c) $\theta = 90$ (d) $\theta = 150$

Fig. 5: High energy and radio emission light curves for $\alpha = 90, \beta = 90, \delta = 90$ with $\epsilon = 0$ and $\epsilon = 0.2R$ for various line of sight angles. The high energy emission curves are shown in red and black for the centred and the off-centred case respectively. Similarly, the green and the blue curves represent the emission curves for the radio regime in the same order.

geometry and the angle of line of sight. Also, the number of peaks for radio emission curve depends on our angle of line of sight and hence, we see one peak in some cases while from both the poles in others. Finally, a significant phase delay is observed between the radio and the high energy light curve for both the cases.

4 Conclusions

We conclude that the off-centred approach is a reliable candidate to be considered while studying pulsars. On comparison of the shape of the polar caps for the offset case with those of the centred one we see significant differences which could help explain various observational signatures. Study of the emission mechanisms with the phase diagrams and the light curves show the differences in the pulse width and phase delay which could give a better insight in our understanding of the emission mechanism. Our next step is to make an analyis of polarization using this approach.

References

Deutsch, A. J. 1955, Annales d'Astrophysique, 18, 1

Gil, J. & Mitra, D. 2001, The Astrophysical Journal, 550, 383, arXiv: astro-ph/0010603

Gil, J. A., Melikidze, G. I., & Mitra, D. 2002, Astronomy and Astrophysics, 388, 235, arXiv: astro-ph/0111474

Gold, T. 1968, Nature, 218, 731

Harding, A. K. & Muslimov, A. G. 2011, The Astrophysical Journal, 743, 181, arXiv: 1111.1668

Hewish, A., Bell, S. J., Pilkington, J. D. H., Scott, P. F., & Collins, R. A. 1968, Nature, 217, 709

Komesaroff, M. M. 1976, Proceedings of the Astronomical Society of Australia, 3, 51

Petri, J. 2015, Monthly Notices of the Royal Astronomical Society, 450, 714, arXiv: 1503.05307

Petri, J. 2016, Monthly Notices of the Royal Astronomical Society, 463, 1240, arXiv: 1608.01015

Radhakrishnan, V. & Cooke, D. J. 1969, Astrophysical Letters, 3, 225

Stift, M. J. 1974, Monthly Notices of the Royal Astronomical Society, 169, 471

Young, M. D., Manchester, R. N., & Johnston, S. 1999, Nature, 400, 848